Journal of the Korean Physical Society, Vol. 74, No. 3, February 2019, pp. 286∼291

X-ray Attenuation Properties of Ultrasmall Yb_2O_3 Nanoparticles as a High-Performance CT Contrast Agent

Adibehalsadat Ghazanfari, Shanti Marasini, Tirusew Tegafaw, Son Long Ho, Xu Miao, Mohammad Yaseen Ahmad, Huan Yue and Gang Ho Lee*

Department of Chemistry and Department of Nanoscience and Nanotechnology (DNN), College of Natural Sciences, Kyungpook National University (KNU), Daegu 41566, Korea

Ji Ae Park and Ki-Hye Jung

Division of RI-Convergence Research, Korea Institute of Radiological & Medical Science (KIRAMS), Seoul 01817, Korea

Yongmin Chang†

Department of Molecular Medicine and Medical & Biological Engineering and DNN, School of Medicine, KNU and Hospital, Daegu 41566, Korea

In Taek Oh and Kwon-Seok Chae

Department of Biology Education and DNN, Teachers' College, KNU, Daegu 41566, Korea

(Received 8 May 2018)

Ultrasmall heavy metal-oxide nanoparticles can be utilized for highly enhancing contrasts in computed tomography (CT). In this study, ultrasmall Yb_2O_3 nanoparticles coated with biocompatible and hydrophilic D-glucuronic acid were for the first time prepared through a simple one-step polyol process, and their X-ray attenuation properties were investigated by measuring phantom images and X-ray attenuation powers. The average particle diameter of the nanoparticles was estimated to be 2.1 ± 0.1 nm by using transmission electron microscopy. The observed X-ray attenuation power was stronger than that of a commercial iodine CT contrast agent (*i.e.*, Ultravist®) at the same atomic concentration and much stronger at the same number density, proving the potential of ultrasmall Yb_2O_3 nanoparticles for use as a powerful CT contrast agent.

PACS numbers: 87.85.Pq, 81.07.Wx, 87.59.−e
Keywords: Yb_2O_3, Ultrasmall nanoparticle, CT contrast agent
DOI: 10.3938/jkps.74.286

I. INTRODUCTION

Ultrasmall heavy metal-oxide nanoparticles can be applied to cutting-edge nanotechnology including nanomedicine [1, 2]. Especially, their application as a computed tomography (CT) contrast agent is promising owing to their strong X-ray attenuation properties originating from the high X-ray attenuation coefficients of heavy metals [3] and the dense population of heavy metals per nanoparticle. Therefore, they can serve as high-performance CT contrast agents that are superior to commercial iodine contrast agents.

Gold (Au) nanoparticles have been most intensively studied so far because of their having higher biocompatibility than other metal nanoparticles [4–18]. However, Au is very expensive, which is a disadvantage of using Au nanoparticles. Therefore, other metal and metal-oxide nanoparticles should be tried as CT contrast agents because they are relatively cheaper than Au nanoparticles.

Yb possesses a high X-ray attenuation coefficient [3]. However, studies on ultrasmall ytterbium-oxide (Yb_2O_3) nanoparticles as CT contrast agents are very poor. The Yb_2O_3 nanoparticles previously reported as CT contrast agents had been prepared at high temperatures through calcination (> 800 °C), and as a result, their particle diameters were large (> 100 nm) (*i.e.*, not ultrasmall) [19,20], which is not appropriate for biomedical applications because they cannot be excreted through the renal system after administration [4]. Furthermore, their surfaces were coated with biocompatible ligands in a separate step. Therefore, their preparation process was very complex.

In this report, we present for the first time a facile

*E-mail: ghlee@mail.knu.ac.kr; Fax: +82-53-950-6330
†E-mail: ychang@knu.ac.kr; Fax: +82-53-420-2677

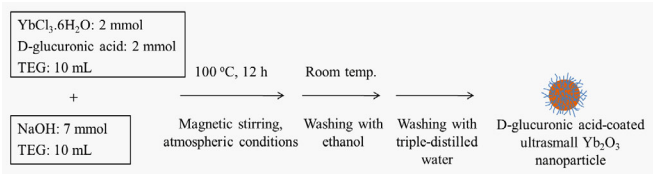

Fig. 1. (Color online) One-step polyol preparation of D-glucuronic acid-coated ultrasmall Yb_2O_3 nanoparticles.

one-step polyol preparation method of ultrasmall Yb_2O_3 nanoparticles [average particle diameter (d_{avg}) = 2.1 ± 0.1 nm] coated with biocompatible and hydrophilic D-glucuronic acid. In this method, nanoparticle formation and surface-coating were accomplished through one-step in solution. The coated nanoparticles were characterized using various experimental techniques. Their X-ray attenuation properties were characterized by measuring phantom images and X-ray attenuation powers. The nanoparticle solution sample exhibited an X-ray attenuation power stronger than that of a commercial iodine CT contrast agent, Ultravist®, proving the potential of such ultrasmall nanoparticles for use as a powerful CT contrast agent.

II. EXPERIMENTAL DETAILS

An outline of the one-step polyol preparation method is provided in Fig. 1. Two separate solutions were prepared: (i) a precursor solution made of 2 mmol of $YbCl_3{\cdot}6H_2O$ and 2 mmol of D-glucuronic acid in 10 mL of triethylene glycol (TEG) in a 100-mL three-necked round bottom flask and (ii) an NaOH solution made of 7 mmol of NaOH in 10 mL of TEG in a 50-mL flask. The three-necked round bottom flask was suspended inside a silicon oil bath for temperature control. The precursor solution was magnetically stirred at room temperature under atmospheric conditions until the precursor was dissolved, after which the NaOH solution was added to the precursor solution. The reaction solution was heated to 100 °C and then maintained at that temperature for 12 h with magnetic stirring. The product solution was cooled to room temperature, transferred to a 1-L beaker, and then filled with 400 mL of ethanol. The product solution was magnetically stirred for 10 min and then kept in a refrigerator for a few days until the product nanoparticles had settled to the bottom of the beaker. The transparent top solution was decanted, and the remaining product solution was diluted with 400 mL of ethanol. This washing process was repeated three times. Half of the sample by volume was dried to a powder form in air for various characterizations, and the remaining half was washed with triple-distilled water three times using the same process as above for the preparation of the aqueous solution sample.

The particle diameter of the nanoparticles was measured using a high-resolution transmission electron microscope (HRTEM) with a field emission filament at an acceleration voltage of 200 kV (Titan G2 ChemiSTEM CS Probe, FEI, Hillsboro, OR, USA). The metal concentration in the aqueous solution sample was measured using an inductively-coupled plasma atomic emission spectrometer (ICPAES) (IRIS/AP, Thermo Jarrell Ash Co., Franklin, MA, USA). A multi-purpose X-ray diffraction (XRD) machine (X'PERT PRO MRD, PANalytical, Almelo, Netherlands) with unfiltered CuK_α radiation (λ = 1.54184 Å) was used to characterize the crystal structure of the powder sample. Fourier transform - infrared (FT-IR) absorption spectra for the powder sample pelletized with KBr were recorded using an FT-IR absorption spectrometer (Galaxy 7020A, Mattson Instruments Inc., Madison, WI, USA) to prove the surface-coating. A thermogravimetric analysis (TGA) instrument (SDT-Q600, TA Instruments, New Castle, DE, USA) was used to estimate the amount of surface coating by recording the TGA curve at temperatures between room temperature and 900 °C under an air flow. The biocompatibility of the aqueous solution sample was determined using a CellTiter-Glo luminescent cell viability assay (Promega, Madison, WI, USA) up to 500 μm [Yb]. Phantom images and X-ray attenuation powers of the aqueous solution sample were measured using a micro-CT scanner (Inveon, Simens Healthcare, Erlangen, Germany). The X-ray attenuation power was estimated in Hounsfield units (HU) with respect to that of water (*i.e.*, 0 HU). The parameters used for the measurement were as follows: X-ray source current = 100 A, X-ray source voltage = 70 kV, imaging time per frame = 200 ms, and reconstructed image size = 512 × 512.

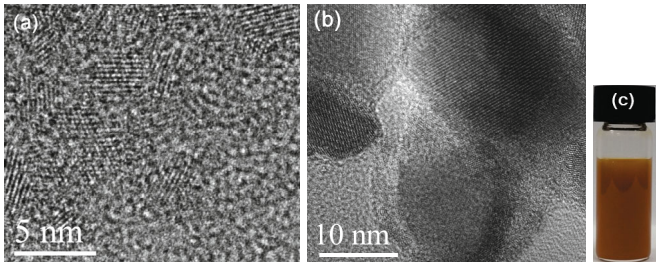

Fig. 2. (Color online) HRTEM images (a) before and (b) after TGA, and (c) a photograph of the D-glucuronic acid-coated ultrasmall Yb_2O_3 nanoparticle solution sample.

III. RESULTS AND DISCUSSION

An HRTEM image of the D-glucuronic acid-coated ultrasmall Yb_2O_3 nanoparticles is shown in Fig. 2(a). The nanoparticles exhibited ultrasmall particle diameters, and their d_{avg} was estimated to be 2.1 ± 0.1 nm (Table 1). After TGA, however, the particle diameters ranged from 10 to 30 nm owing to particle growth, as

Table 1. Average particle diameter (d_{avg}), number (N_{metal}) of Yb^{3+} ions per nanoparticle, surface-coating amount (P, σ, N_{ligand}), and X-ray attenuation power relative to Ultravist®.

d_{avg} (nm)	N_{metal}	Surface-coating amount			X-ray attenuation power relative to Ultravist®	
		P (%)	σ (nm^{-2})	N_{ligand}	In atomic concentration	In number density
2.1 ± 0.1	~ 297	44.9 ± 1.0	9.1 ± 0.1	126 ± 10	~ 1.8	~ 180

P = weight percent of surface-coated D-glucuronic acid per nanoparticle.
σ = grafting density, corresponding to the number of surface-coated D-glucuronic acid molecules per nanoparticle unit surface area.
N_{ligand} = number of surface-coated D-glucuronic acid molecules per nanoparticle.

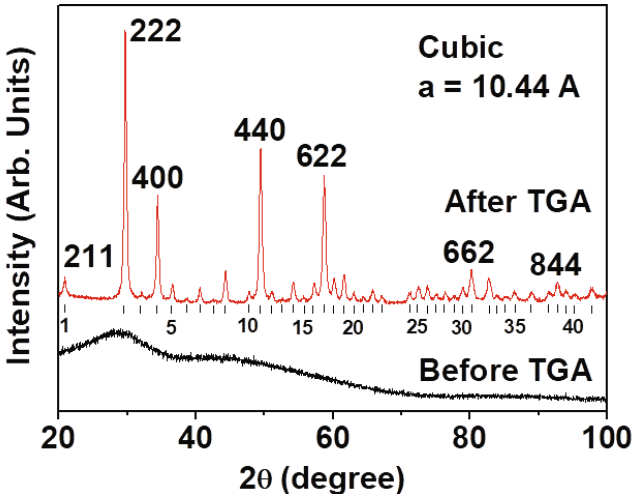

Fig. 3. (Color online) XRD patterns of the D-glucuronic acid-coated ultrasmall Yb_2O_3 nanoparticle powder sample before (bottom) and after (top) TGA. All the peaks of the top XRD pattern labeled with vertical sticks and Arabic numbers could be assigned with (hkl) Miller indices. Only the strong peaks were representatively assigned on the top of the peaks.

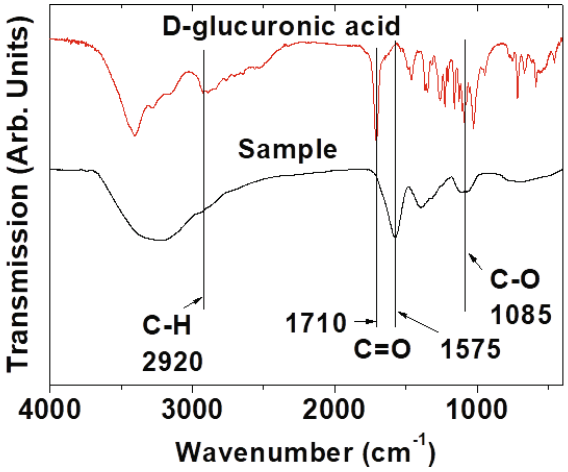

Fig. 4. (Color online) FT-IR absorption spectra of free D-glucuronic acid and a D-glucuronic acid-coated ultrasmall Yb_2O_3 nanoparticle powder sample.

shown in Fig. 2(b). The aqueous solution sample exhibited a good colloidal suspension [Fig. 2(c)], which is suitable for application as a CT contrast agent.

The XRD pattern of the powder sample was measured before and after TGA (Fig. 3). Broad and amorphous peaks were observed for the powder sample before TGA (the bottom XRD pattern in Fig. 3) whereas sharp peaks were observed owing to particle growth after TGA (the top XRD pattern in Fig. 3), which is consistent with the HRTEM result shown in Fig. 2(b). All the peaks after TGA could be assigned with (hkl) Miller indices, and only the strong peaks were representatively assigned in the XRD pattern. After TGA, the Yb_2O_3 nanoparticles showed a cubic structure with a lattice constant (a) of 10.44 ± 0.01 Å, which is consistent with the previously reported value (JCPDS card No. 00-043-1037 [21]).

Surface-coating with D-glucuronic acid was investigated by recording the FT-IR absorption spectrum (Fig. 4). The FT-IR absorption spectrum of free D-glucuronic acid was also recorded for reference (Fig. 4). The characteristic IR bands of C−H at 2920 cm^{-1}, C=O at 1575 cm^{-1}, and C−O at 1085 cm^{-1} were observed in the sample. A red-shift of the C=O band by 135 cm^{-1} with respect to that (= 1710 cm^{-1}) of free D-glucuronic acid was observed owing to the electrostatic bonding of the −COOH group of D-glucuronic acid to the Yb^{3+} exposed on the nanoparticle surface. Similar red-shifts have previously been observed in many nanoparticle systems coated with ligands containing −COOH groups [22–25], supporting our results.

The average amount (P) of surface-coated D-glucuronic acid on the nanoparticle surface was estimated in units of weight percent by measuring the mass loss in the TGA curve, after considering the water and air desorption at temperatures between room temperature and $\sim$ 105 °C (Fig. 5). The grafting density (σ), corresponding to the average number of surface-coated D-glucuronic acid molecules per nanoparticle unit surface area [26], was estimated using the bulk density of Yb_2O_3 (= 9.17 gcm^{-3}) [27], the estimated P value, and the d_{avg} as determined via HRTEM imaging. The average number (N_{ligand}) of surface-coated D-glucuronic acid molecules per nanoparticle was estimated by multiplying the σ value by the nanoparticle surface area (= πd_{avg}^2). The estimated P, σ, and N_{ligand} values are provided in Table 1. The large value of the N_{ligand} indicates that the

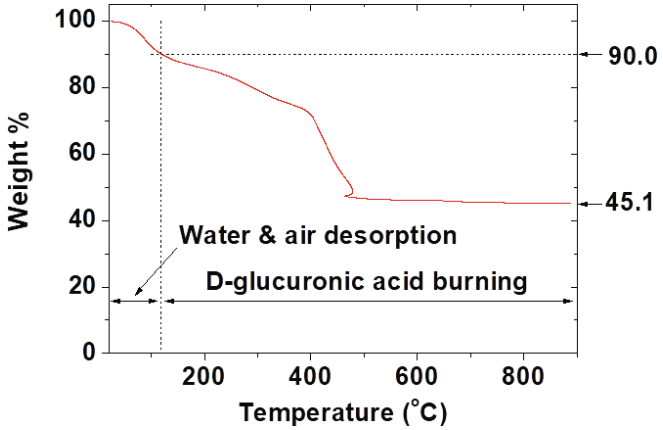

Fig. 5. (Color online) TGA curve for the D-glucuronic acid-coated ultrasmall Yb_2O_3 nanoparticle powder sample.

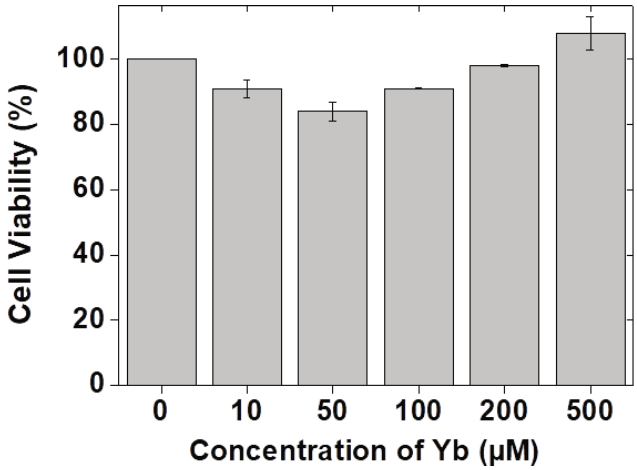

Fig. 6. In vitro cellular cytotoxicity of the D-glucuronic acid-coated ultrasmall Yb_2O_3 nanoparticle solution sample in DU145 cells, showing good biocompatibility up to 500 μM [Yb].

nanoparticles were coated with a sufficient amount of D-glucuronic acid. As shown in Fig. 6, D-glucuronic acid-coated ultrasmall Yb_2O_3 nanoparticles were not toxic up to 500 μm [Yb] in DU145 cells, showing good biocompatibility.

The X-ray attenuation properties of the nanoparticle solution sample were characterized by measuring phantom images and X-ray attenuation powers in HU. The results were compared with those of Ultravist®. As shown in Fig. 7(a), the nanoparticle solution sample exhibited a phantom image that was brighter than the Ultravist® image at the same atomic concentration. This was also indicated in the plot of the X-ray attenuation power as a function of the atomic concentration shown in Fig. 7(b), which is consistent with the magnitudes of the atomic X-ray attenuation coefficients (*i.e.*, Yb > I) [3]. From the plot, the X-ray attenuation power of the D-glucuronic acid-coated ultrasmall Yb_2O_3 nanoparticles was estimated to be ∼ 1.8 times stronger than that of

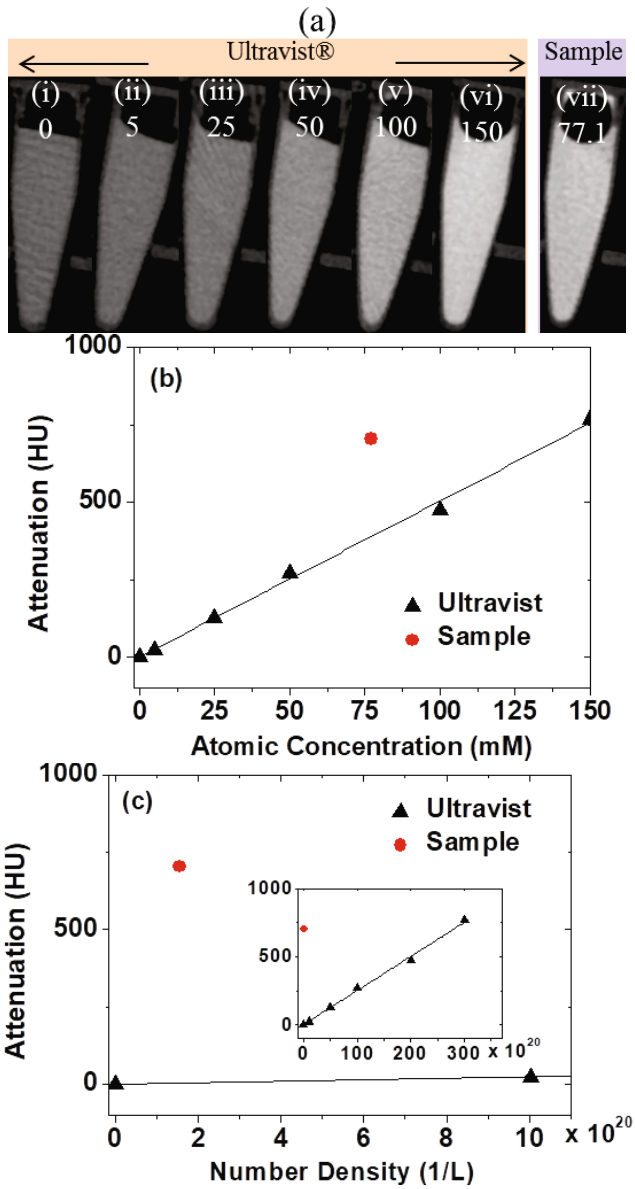

Fig. 7. (Color online) (a) Phantom images of (i) - (vi) Ultravist® (0 - 150 mM [I]) and (vii) the D-glucuronic acid-coated ultrasmall Yb_2O_3 nanoparticle solution sample (77.1 mM [Yb]). Plots of the X-ray attenuation power as a function of (b) the atomic concentration and (c) the number density. In (c), a reduced range of $0 - 10 \times 10^{20}$ was plotted, and the inset corresponds to a plot over the entire range.

Ultravist® at the same atomic concentration (Table 1).

To plot the X-ray attenuation power as a function of the number density corresponding to the number of nanoparticles (or molecules) per liter, we estimated the number (N_{metal}) of Yb^{3+} ions per nanoparticle to be ∼ 297 by using the formula [28] $N_{\mathrm{metal}} =\sim (x/y)(d_{\mathrm{avg}}/h)^3$, in which x (= 2) is the number of Yb^{3+} ions per chemical formula, y (= 5) is the number of ions per chemical formula, and h is the average ionic diameter of all the ions in the chemical formula (= 0.232 nm) [29]. The es-

timated value is also provided in Table 1. By multiplying the atomic concentration by Avogadro's number and then dividing the resulting number either by N_{metal} or by three in the case of Ultravist® (*i.e.*, three iodines per molecule), we obtained the corresponding number density. The X-ray attenuation power was then plotted as a function of the number density [Fig. 7(c)]. From the plot, the X-ray attenuation power of the D-glucuronic acid-coated ultrasmall Yb_2O_3 nanoparticles was estimated to be 180 times stronger than that of Ultravist® at the same number density (Table 1), and this value was 100 times bigger than that ($=\sim 1.8$) estimated at the same atomic concentration, corresponding to an advantage of ultrasmall nanoparticle CT contrast agents over molecular ones. Therefore, the ultrasmall Yb_2O_3 nanoparticles are superior to commercial iodine CT contrast agents.

IV. CONCLUSION

In summary, we prepared for the first time ultrasmall Yb_2O_3 nanoparticles coated with D-glucuronic acid through an one-step polyol process and characterized their potential for use as CT contrast agent by measuring phantom images and X-ray attenuation powers. The results are as follows:

(1) D-glucuronic acid-coated ultrasmall Yb_2O_3 ($d_{\mathrm{avg}} = 2.1 \pm 0.1$ nm) nanoparticles showed good biocompatibility according to the in vitro cellular cytotoxicity assessment.

(2) The nanoparticle solution sample showed an X-ray attenuation power that was stronger than that of a commercial iodine contrast agent, Ultravist®, which is consistent with the magnitudes of the atomic X-ray attenuation coefficients (*i.e.*, Yb > I).

(3) The X-ray attenuation power of the nanoparticle solution sample was much stronger than that of Ultravist® at the same number density, proving the superiority of the ultrasmall Yb_2O_3 nanoparticles to commercial iodine CT contrast agents.

ACKNOWLEDGMENTS

This study was supported by the Basic Science Research Program (Grant No. 2017R1A2B3003214 to YC and 2016R1D1A3B01007622 to GHL) and the Basic Research Laboratory (BRL) Program (Grant No. 2013R1A4A1069507) of the National Research Foundation funded by the Ministry of Education, Science, and Technology, South Korea. The authors wish to thank the Korea Basic Science Institute for providing their XRD spectrometer.

REFERENCES

[1] A. Umar and Y-B. Hahn, *Metal Oxide Nanostructures and Their Applications* (American Scientific Publishers, Valencia, CA, USA, 2010).
[2] E. Matijević, *Fine Particles in Medicine and Pharmacy* (Springer, Boston, MA, USA, 2012).
[3] J. H. Hubbell and S. M. Seltzer, *Tables of X-Ray Mass Attenuation Coefficients and Mass Energy-Absorption Coefficients from 1 keV to 20 MeV for Elements Z = 1 to 92 and 48 Additional Substances of Dosimetric Interest* (Gaithersburg, NIST, USA, 1996).
[4] J. F. Hainfeld, D. N. Slatkin, T. M. Focella and H. M. Smilowitz, Br. J. Radiol. **79**, 248 (2006).
[5] S. Ahn, S. Y. Jung and S. J. Lee, Molecules **18**, 5858 (2013).
[6] C. C. Chien, H-H. Chen, S-F. Lai, K-C. Wu, X. Cai, Y. Hwu, C. Petibois, Y. Chu and G. Margaritondo, J. Nanobiotechnol. **10**, 10 (2012).
[7] K. T. Butterworth, S. J. McMahon, F. J. Currell and K. M. Prise, Nanoscale **4**, 4830 (2012).
[8] J. Li, A. Chaudhary, S. J. Chmura, C. Pelizzari, T. Rajh, C. Wietholt, M. Kurtoglu and B. Aydogan, Phys. Med. Biol. **55**, 4389 (2010).
[9] D. P. Cormode, E. Roessl, A. Thran, T. Skajaa, R. E. Gordan, J-P. Schlomka, V. Fuster, E. A. Fisher, W. J. Mulder, R. Proksa and Z. A. Fayad, Radiology **256**, 774 (2010).
[10] D. Kim, S. Park, J. H. Lee, Y. Y. Jeong and S. Jon, J. Am. Chem. Soc. **129**, 7661 (2007).
[11] D. Xi, S. Dong, X. Meng, Q. Lu, L. Meng and J. Ye, RSC Adv. **2**, 12515 (2012).
[12] V. Kattumuri, K. Katti, S. Bhaskaran, E. J. Boote, S. W. Casteel, G. M. Fent, D. J. Robertson, M. Chandrasekhar, R. Kannan and K. V. Katti, Small **3**, 333 (2007).
[13] I-C. Sun, D-K. Eun, J. H. Na, S. Lee, I-J. Kim, I-C. Youn, C-Y. Ko, H-S. Kim, D. Lim, K. Choi, P. B. Messersmith, T. G. Park, S. Y. Kim, I. C. Kwon, K. Kim and C-H. Ahn, Chem. Eur. J. **15**, 13341 (2009).
[14] C. Kojima, Y. Umeda, M. Ogawa, A. Harada, Y. Magata and K. Kono, Nanotechnology **21**, 245104 (2010).
[15] R. Popovtzer, A. Agrawal, N. A. Kotov, A. Popovtzer, J. Balter, T. E. Carey and R. Kopelman, Nano Lett. **8**, 4593 (2008).
[16] C. Xu, G. A. Tung and S. Sun, Chem. Mater. **20**, 4167 (2008).
[17] P. Huang, L. Bao, C. Zhang, J. Lin, T. Luo, D. Yang, M. He, Z. Li, G. Gao, B. Gao, S. Fu and D. Cui, Biomaterials **32**, 9796 (2011).
[18] C. Alric, J. Taleb, G. L. Duc, C. Mandon, C. Billotey, A. L. Meur-Herland, T. Brochard, F. Vocanson, M. Janier, P. Perriat, S. Roux and O. Tillement, J. Am. Chem. Soc. **130**, 5908 (2008).
[19] Z. Liu, Z. Li, J. Liu, S. Gu, Q. Yuan, J. Ren and X. Qu, Biomaterials **33**, 6748 (2012).
[20] Z. Liu, F. Pu, J. Liu, L. Jiang, Q. Yuan, Z. Li, J. Ren and X. Qu, Nanoscale **5**, 4252 (2013).
[21] Card No. 00-043-1037, X'Pert High Score, PANalytical software (Almelo, The Netherlands, 1998), Ver. 1.1.
[22] O. W. Duckworth and S. T. Martin, Geochim. Cosmochim. Acta **65**, 4289 (2001).
[23] S. J. Hug and D. Bahnemann, J. Electron Spectrosc. Relat. Phenom. **150**, 208 (2006).

[24] S. J. Hug and B. Sulzberger, Langmuir **10**, 3587 (1994).
[25] C. B. Mendive, T. Bredow, M. A. Blesa and D. W. Bahnemann, Phys. Chem. Chem. Phys. **8**, 3232 (2006).
[26] M. K. Corbierre, N. S. Cameron and R. B. Lennox, Langmuir **20**, 2867 (2004).
[27] R. C. Weast, M. J. Astle and W. H. Beyer, *CRC Handbook of Chemistry and Physics* (CRC Press, Inc., Boca Raton, FL, USA, 1984-1985), p. B-158.
[28] S. J. Kim, W. Xu, M. W. Ahmad, J. S. Baeck, Y. Chang, J. E. Bae, K. S. Chae, T. J. Kim, J. A. Park and G. H. Lee, Sci. Technol. Adv. Mater. **16**, 055003 (2015).
[29] J. A. Dean, *Lange's Handbook of Chemistry* (McGraw-Hill, New York, USA, 1992), p. 4.15 for O^{2-} and p. 4.17 for Yb^{3+}.